

Article

Chlorophyll Fluorescence Imaging (CFI) and Laser-Induced Breakdown Spectroscopy (LIBS) Applied to Investigate Tomato Plants Infected by the Root Knot Nematode (RKN) *Meloidogyne incognita* and Tobacco Plants Infected by Cymbidium Ringspot Virus

Giorgio Saverio Senesi ^{1,*}, Olga De Pascale ¹, Bruno Spolon Marangoni ², Anderson Rodrigues Lima Caires ², Gustavo Nicolodelli ³, Vitantonio Pantaleo ⁴ and Paola Leonetti ^{4,*}

¹ CNR, Institute for Plasma Science and Technology (ISTP), Research Unit of Bari, 70126 Bari, Italy

² Physics Institute, Federal University of Mato Grosso do Sul, Campo Grande 79070-900, MS, Brazil

³ Departamento de Física, Federal University of Santa Catarina, Florianopolis 88040-900, SC, Brazil

⁴ CNR, Institute for Sustainable Plant Protection (IPSP), Research Unit of Bari, 70126 Bari, Italy

* Correspondence: giorgio.senesi@cnr.it (G.S.S.); paola.leonetti@cnr.it (P.L.)



Citation: Senesi, G.S.; De Pascale, O.; Marangoni, B.S.; Caires, A.R.L.; Nicolodelli, G.; Pantaleo, V.; Leonetti, P. Chlorophyll Fluorescence Imaging (CFI) and Laser-Induced Breakdown Spectroscopy (LIBS) Applied to Investigate Tomato Plants Infected by the Root Knot Nematode (RKN) *Meloidogyne incognita* and Tobacco Plants Infected by Cymbidium Ringspot Virus. *Photonics* **2022**, *9*, 627. <https://doi.org/10.3390/photonics9090627>

Received: 21 July 2022

Accepted: 30 August 2022

Published: 1 September 2022

Publisher's Note: MDPI stays neutral with regard to jurisdictional claims in published maps and institutional affiliations.



Copyright: © 2022 by the authors. Licensee MDPI, Basel, Switzerland. This article is an open access article distributed under the terms and conditions of the Creative Commons Attribution (CC BY) license (<https://creativecommons.org/licenses/by/4.0/>).

Abstract: Recently, studies on climate change have highlighted the central role of photosynthetic mechanisms in the defense response of plants to abiotic and biotic stresses. Photo-sensing and photo-activation are innovative technologies applied for the early detection of plant pathogens in order to prevent the dramatic impact they may have on plants. Chlorophyll Fluorescence Imaging (CFI) and Laser-Induced Breakdown Spectroscopy (LIBS) analytical techniques can be used to evaluate the amount of chlorophyll in plants, which can be altered in the case of biotic and abiotic stresses. In this work, both techniques were applied to two pathogenic model systems, i.e., roots of susceptible tomato plants infected by *Meloidogyne incognita* and *Nicotiana benthamiana* plants infected by cymbidium ringspot virus. Experimental evidence is provided and discussed showing that specific application protocols of both methods can be used successfully for the early detection of symptoms of the pathogen attacks of *Meloidogyne incognita* on tomato roots and of cymbidium ringspot virus infected plants. In particular, a decrease in chlorophyll content was measured by fluorescence imaging, and an increase in Mg⁺⁺ content was determined by LIBS in both the leaves and stems of infected tomato plants and the leaves of infected plants, with respect to control (non-infected) plants. Thus, the two techniques used have been shown to be able to discriminate satisfactorily between control and infected plants and to provide some insight on the underlying mechanisms of plant defenses against nematodes and viruses.

Keywords: tomato; *Meloidogyne incognita* root knot nematode; tobacco; cymbidium ringspot virus; chlorophyll fluorescence imaging; laser-induced breakdown spectroscopy

1. Introduction

The interactions between host plants and viruses or phytoparasitic nematodes affect plant productivity and tolerance to biotic and abiotic stresses.

Nowadays, a matter of general concern is how invasive the impact of climate change is on biodiversity and complex systems [1]. In particular, efforts are being made to address challenges arising from abiotic (drought, salt and heat) and biotic (diseases) stress conditions related to food chain production and affecting agriculture and plant health. Plants under biotic stress, including those induced by fungi, phytoparasitic nematodes and viruses, produce molecules, substances and signals as defense responses. A wide range of literature of considerable scientific impact has shown that localized attacks by either root pathogens or local mechanical wounds induce a systemic production of molecules

acting as hormones, e.g., salicylic acid (SA) and jasmonic acid (JA), and signal molecules of various origins.

With the emergence of precision agriculture, the development and implementation of fast and reproducible methods to detect the pathogen attack as early as possible have become increasingly important to prevent the loss of production. Both hormone and signal molecules would be relevant means of the plant defense mechanisms acting to limit the availability of nutrients to pathogens and their capacity of harnessing the plant metabolism to their advantage. The complexity of these interactions must be considered duly in studies of host plant resistance to pathogen attacks. Root knot nematodes (RKN) are soil-borne root pathogens that can attack many crops of high economic interest, thereby having a devastating impact on agriculture worldwide. Currently, the root apparatus of tomato (*Solanum lycopersicum* L.) infected by the *Meloidogyne incognita* spp. is one of the best systems to study plant–parasitic nematode interactions. This phytoparasitic nematode is particularly interesting as its complete genome has been released for public research, which has thus opened the possibility to extend the basic studies to infer new biotechnologies for its control and possible extension to other plants of agricultural interest [2,3]. Pioneering studies [4,5] have shown that the respiration and intermediary metabolism in roots of the model plant *A. thaliana* inoculated with RKN alter the chlorophyll content in the aerial parts of the plant, so that the rate of photosynthesis can be easily detected by innovative technologies.

Plant viruses are also widespread pathogens that have a major impact on agroecosystems and the agro-food industry. The tomato mosaic virus (ToMV) belonging to the Tobamovirus genus was used in the CRISPR/Cas12a-based, sequence-specific detection of quarantine plant viruses, as it features a high destructive potential and capacity for transmission by mechanical contact involving hands, tools, soil and parts of infected plants, and whose detection and control is a major issue for seed companies due to the characteristic transmissibility from seeds [6]. For all these reasons, efforts have been spent to detect the viral pathogen and disease by imaging techniques [7,8] and optical methods, including fluorescence, multispectral and hyperspectral imaging, and thermography [9]. The main advantage of optical methods is that they can detect changes occurring in the plant during the pathogen–host interaction. Other advantages of these techniques are the non-invasiveness, high sensitivity and high analytical speed. Specifically for plants, green leaves can be used to investigate the physiological status of plants by monitoring their chlorophyll fluorescence or blue-green fluorescence, contributing, for instance, to the early identification of any type of impairment resulting from major nutrient deficiencies [10].

In particular, Tauseef et al. [11] evaluated the role of different concentrations (0, 25, 50 or 100 ppm) of Mg and the modes of application (root dip, soil drench, foliar spray) of MgO nanoparticles on cowpea infected with *M. incognita*. A 100 ppm dose of MgO nanoparticles applied as root dip resulted in reduced nematode fecundity, a decreased number and smaller size of galls, enhanced plant growth, and increased chlorophyll, carotenoid, seed protein and root and shoot N contents. Thus, MgO nanoparticles played a twin role, both as a nematicidal agent and as a growth promotion inducer. In the same year, Brouwer et al. [12] found distinctly different distribution patterns of accumulation at the site of inoculation in the resistant lines for Ca, Mg, Mn and Si compared to the susceptible cultivar. The results revealed different ionomes in diseased plants compared to resistant plants. However, our studies will be continued, possibly extending the use of our methods to other not only susceptible but also resistant plants, and to other models of interaction such as cyst nematodes–host plants and nematodes–plant fungi [13].

Laser-Induced Breakdown Spectroscopy (LIBS) is a type of atomic emission spectrometry based on plasma generation by high power pulses which, in recent decades, has become a popular analytical technique in several fields of research. This is thanks to its unique features such as a wide applicability, no or minimal sample preparation, capability of multi-elemental analysis, no waste production, rapidity, affordable costs and remote

sensing capability. Further, LIBS is particularly attractive because of the availability of portable equipment, enabling in situ and on-line measurements [14].

In the last decade, LIBS has been applied widely in the food sector (fruits and grains) and for the detection of plant diseases [15–19]. LIBS has contributed successfully to achieving the early diagnosis of citrus, soybean and tobacco diseases. In an early study, Pereira et al. [20] applied LIBS associated with SIMCA to direct measurement without any pretreatment of the organic and inorganic signal profiles of citrus plant leaves, either healthy or inoculated with the bacterium *Candidatus Liberibacter asiaticus* (CLas). As a result, citrus samples in the first month of inoculation could be discriminated amongst, with 97% correct predictions. Some years later, Sankaran et al. [21] applied LIBS to citrus leaves for the rapid and real-time detection of various anomalies, including the Huanglongbing (HLB) bacterial destructive disease, citrus cancer and nutrient deficiencies from Fe, Mn, Mg and Zn. Peng et al. [22] proposed a novel approach based on LIBS to discriminate between tobacco leaves infected by the tobacco mosaic virus (TMV, a relative of ToMV) and healthy leaves. The application of the PLS-DA model to LIBS spectral data acquired on both fresh and dried pelletized leaves provided good discrimination only in the case of dried leaves. Recently, Ranulfi et al. [23] attempted to evaluate LIBS by the elemental compositional factors related to the syndrome denoted as “green stem and foliar retention”, commonly known as “soya louca II” (mad soy II), caused by the nematode *Aphelenchoides besseyi* in soybean plants, whose symptoms are possibly ascribed to the unbalance of the macronutrients Ca, K and Mg. The content of these elements was measured by LIBS and atomic absorption spectrometry (AAS) as the reference technique, in leaves collected from healthy and disease-affected soybean plants of two varieties. Higher Ca and Mg contents were measured in the leaves of healthy plants, whereas a higher K content could be ascribed to the development of the disease. Furthermore, LIBS data analysis by classification via regression (CVR) and partial least square regression (PLSR) cross validation methods yielded success rates higher than 80% in class differentiation.

The aim of this work was to test the performance of two distinct techniques, i.e., chlorophyll fluorescence imaging (CFI) and LIBS, in the study of two systems, such as tomato-RKN nematode and *Nicotiana benthamiana* (hereafter “tobacco”)-cymbidium ringspot virus (CymRSV, member of the genus *Tombusvirus*, Family *Tombusviridae*), a plant virus model available in our lab, in order to provide a quick answer on the progress of the pathogen’s attack on the host plant. The first system refers to an attack of a pathogenic type, i.e., while infecting the root system, the infection weakens the plant so much as to affect its fitness, the appearance of leaves, and the possibility of producing fruit. The second system refers to an attack that produces symptoms directly on the foliar apparatus. The combined use of the two techniques is based on the complementarity of information provided. LIBS is a technique that detects atomic transitions, thus providing data on the elemental composition of the plant, whereas fluorescence detects molecular transitions, i.e., the molecular composition. In particular, CFI provides information on the chlorophyll content, which is closely related with the photosynthetic performance of the plant. Therefore, LIBS and CFI yield complementary information, i.e., LIBS can inform on the changes of plants’ elemental composition caused by the plant virus, and CFI reveals how the plant virus impacts the physiological status of the plants, and in particular, its photosynthetic capacity when infected.

2. Materials and Methods

2.1. Tomato Plant and Phytoparasitic Nematode

Seeds of the tomato (*Solanum lycopersicon* L.) cultivar Roma VF, a variety fully susceptible to RKNs, were used in the experiments [24,25]. The seeds were surface sterilized and sown in a sterilized mixture of peat and soil at 23–25 °C in a glasshouse. Single tomato seedlings were then transplanted into 100 cm³ clay pots filled with steam-sterilized river sand and allowed to grow to the fifth–sixth leaf stage. Pots were randomly placed on temperature-controlled (23–25 °C) benches located in a glasshouse (Figure 1).

A freshly infective juvenile larvae (J2s) of *M. incognita* collected from egg masses of infested tomato roots, and held to hatch in a growth chamber at 25 °C, were used to inoculate tomato plants. Susceptible plants were inoculated with 300 J2s per plant, which penetrated and established into the roots, as checked with a stereoscope, 21 days after inoculation [26]. The presence of the symptoms of the attack (galls) was verified by observation with a Leica M125 stereomicroscope. At this time, the leaves, stems and roots were collected and analyzed by CFI, LIBS and a biochemical assay for chlorophyll content measurement.



Figure 1. Inoculum of J2 (a) and CymRSV virus (b), a tomato plant (c), a tobacco plant (d), and healthy and infected plants in the growth chamber (e).

2.2. Tobacco Plant and Cymbidium Ringspot Virus

The infection level was tested using three replicates for each experiment and three leaves were collected from each plant replicate (number of samples, $n = 9$). Three subsequent experiments were carried out with three replications each. The leaves collected from six-leave-old seedlings of *Nicotiana benthamiana* were mechanically inoculated by the CymRSV. A total of 15 days after inoculation, the water extracts of some leaves were analyzed by transmission electron microscopy (TEM) with a Morgagni 282D (Philips, Amsterdam, The Netherlands) for morphological virus characterization, and the other leaves were analyzed by CIF and LIBS. The values are expressed as means $n \pm$ standard deviation for virus-infected tobacco leaves and control plants.

2.3. Chlorophyll Fluorescence Imaging (CFI)

The CFI experiments were performed using a Fluorescence Imaging System (FluorCam FC 800-O/1010-GFP, Photon Systems Instruments, Drásov, Czech Republic) consisting of two panels with blue LEDs (470 nm), for providing a saturating pulse of up to $6000 \mu\text{mol}/\text{m}^2 \text{s}^1$, and two panels of red LEDs (618 nm) with an intensity of $200 \mu\text{mol}/\text{m}^2 \text{s}^1$, to be used as measuring light. A progressive scanning couple charge device (CCD) camera was used to collect the fluorescence images with a resolution of 1024×768 pixels. Before imaging collection, the plants were adapted to the dark for 20 min to ensure that all chlorophyll molecules were in the ground state, and consequently, that no photosynthesis occurred prior to the measurement. Then, the maximum fluorescence (F_m) images of the plants, in a dark-adapted state, were obtained by applying a saturating pulse of $4000 \mu\text{mol}/\text{m}^2 \text{s}^1$. An optical filter selected only the chlorophyll emission in the region around 695 nm. The fluorescence image measurements were performed on plants previously removed from the vessels.

2.4. Laser-Induced Breakdown Spectroscopy (LIBS)

The LIBS apparatus used in this experiment was a self-assembled system composed of a Nd:Yag Q-switched laser operating at a 1064 nm wavelength with a 6 ns pulse duration and maximum energy of 200 mJ per pulse. The beam was focused onto a 50 μm spot diameter of the sample, which resulted in a power density of approximately 2×10^{12} W/cm². The plasma light was captured by a Stellarnet spectrometer operating in the spectral range 190–300 nm with a 0.2 nm optical resolution. The delay time between the laser shot and spectrum acquisition was 500 ns, and the spectrometer integration time was 1 μs . The measurements were performed on fresh leaf, root and stem samples with no preparation. The spectra were recorded by averaging two consecutive shots. For each sample, 20 spectra were acquired and averaged.

To eliminate non-standard outliers, the experimental spectra were subjected to an outlier exclusion process using the spectral angle mapper (SAM) routine [27,28]. This method treats each spectrum as one vector, calculating the scalar product between two spectra. The normalized result returns the cosine value between the vectors, which is a value between -1 and 1 , indicating similarity the closer the value is to 1 . Then, an algorithm automatically eliminates spectra that are very different from the others, i.e., with average similarity values lower than 0.9 in our case. The rate of excluded spectra was less than 5% .

2.5. Multivariate Analysis

The LIBS spectra were subjected to a dimensionality reduction process by principal component analysis (PCA). PCA is an unsupervised linear and orthogonal transformation process that reduces the initial number of variables into a set of uncorrelated variables. This new set of data, called principal components (PC), maintains most of the original variation of the system, allowing for the visualization of clusterization in a simple graphical plot [29] and increasing the efficiency of the further application of supervised machine learning algorithms [30].

Then, supervised machine learning routines were applied to train the dataset and develop a model. The algorithms were based on discriminant analysis (DA), support vector machine (SVM) and K-nearest neighbor (KNN). The number of PCs used in each training test guaranteed a minimum of 95% of the total variance of the original system.

The DA algorithm uses the training data to define a more adequate contour that separates the established classes, classifying an unknown sample according to the training criterion. The SVM organizes the data into a spatial distribution by dividing the classes by hyperplanes, which can be linear or non-linear and are adjusted to the training data to achieve the best performance. The KNN is based on the spatial distribution of data, and classifies the sample based on the nearest neighbors. The algorithm can be optimized by the number and distance (euclidean or weighted) of the nearest neighbors.

In the last step a validation process was performed. As the number of samples in our set is small, it was applied the leave one out cross validation (LOOCV) method, i.e., a sample taken from the training set and used later to test the model. The predicted class is then compared to its true class. The result is then recorded in a confusion matrix. The process is repeated so as to validate all samples in the set. At the end, we obtain the model accuracy, i.e., the correct predictions in relation to the total of samples.

2.6. Chlorophyll Measurement

Tomato leaf samples were harvested from control and infected plants and stored in liquid nitrogen in the dark at 80°C . Subsequently, chlorophyll a (Chl a) and b (Chl b) were extracted using an 80% acetone solution. The absorbance at the wavelengths of 663 nm and 648 nm was measured with a Beckman Coulter DU[®] 800 Spectrophotometer. The concentrations of chlorophylls were calculated according to Porra et al. [31]. Nine different sections from different leaves were randomly measured, and the mean value ($\pm\text{SE}$) of three biological replicates was considered.

3. Results and discussion

3.1. Tomato Leaves, Stems and Roots

The comparison of chlorophyll a and chlorophyll b contents in the leaves from the control and infected tomato plants clearly shows that the attack of the J2 of *M. incognita* induces a decrease in the content of both chlorophylls (Figure 2).

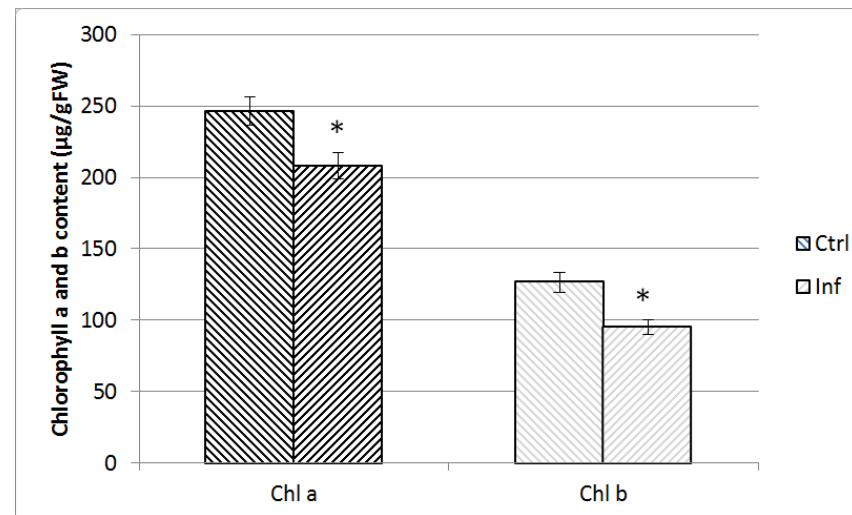


Figure 2. Contents of chlorophyll a (Chl a) and chlorophyll b (Chl b) in the control (Ctrl) and infected (Inf) tomato leaves. The asterisks on the column indicate a highly significant difference between the two treatments (Ctrl and Inf) at the nematode infestation time (t -test; * $p < 0.05$).

Only tomato leaves and stems were analyzed by CFI, whereas the roots were not, as they do not present a significant amount of chlorophyll. The fluorescence images of tomato leaves clearly show a chlorophyll content decrease in the infected sample with respect to the control one (Figure 3).

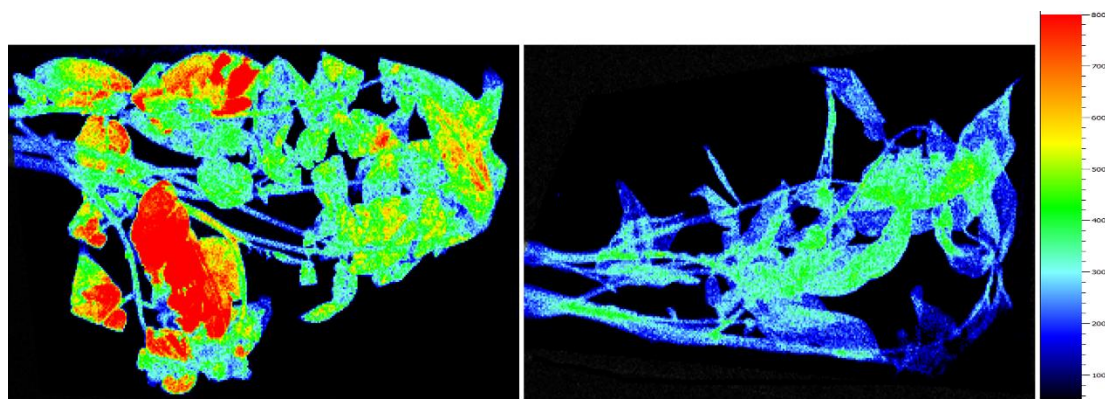


Figure 3. Fluorescence images (F_m measurements) of control (left) and *M. incognita*-infected (right) tomato leaves.

A similar behavior was previously detected in the leaves of *Vitis vinifera* infected by the same nematode, which also showed a significant decrease in total respiration, photosynthesis, energy assimilated into plant tissues, respiration and gross production efficiency [32]. In greenhouse tests, Lu et al. [33] evaluated the extent to which moderate or high levels of resistance to *M. incognita* infection influenced the growth and physiology of cotton plants by measuring the height-to-node ratio, chlorophyll content, dark-adapted quantum yield of photosystem II and leaf area. Achieved results confirmed the previous ones, i.e., that the infection by *M. incognita* was associated with a reduced chlorophyll content and a reduction in resistant genotypes similar to that of susceptible genotypes.

Recently, Udalova et al. [34] have shown that the production of hormones such as salicylic acid and reactive oxygen species (ROS) by the host plant in response to the attack of the RKN *M. incognita* on the roots is connected with the level of photosynthetic processes that occur in the leaves. Successively, Udalova et al. [35] provided stronger evidence of the correlation between ROS and photorespiration and photosynthesis. Furthermore, biochemical approaches demonstrated that the increase in ROS in tomato roots infected by *M. incognita* is activated as a consequence of the defense responses of the host plant [25,36,37]. These results validate the well-known mechanisms of plant–nematode interaction and confirm the efficiency of the fast and repeatable CFI method for its use, for example, in precision agriculture, being able to indicate at an early stage the possibility of damage to the newly formed root system.

Figure 4 shows a typical LIBS spectrum of uninfected tomato fresh leaf (control) compared with that of a tomato fresh leaf whose roots were infected by *M. incognita*. Four atomic and ionic emission lines were detected in the spectral range from 190 to 300 nm, which were assigned, based on the NIST database [38], to C I at 193.03 and 247.86 nm, Mg II at 280.34 nm and Mg I at 285.31 nm. The comparison of LIBS emission line intensities showed a higher intensity for the Mg⁺⁺ lines in the infected plant with respect to the control ones, while the intensities for C lines remained the same in both samples (Figure 4).

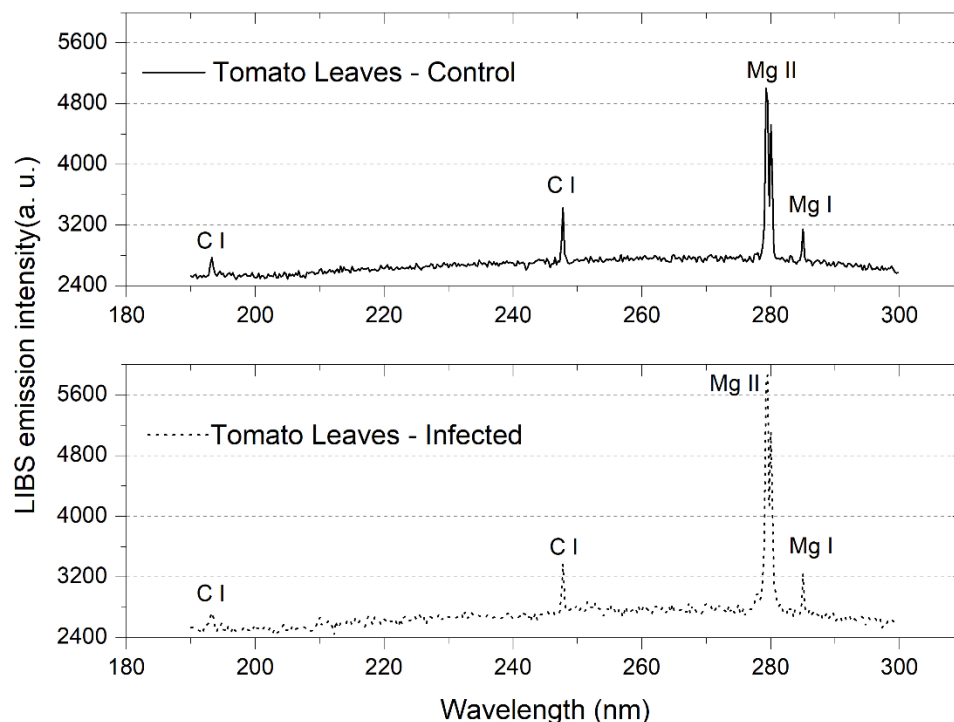


Figure 4. LIBS spectra of tomato leaves of uninfected plants and plants with roots infected by *M. incognita*.

The role of elements such as C and Mg⁺⁺ in plants is too complex to allow for a simple interpretation, as this ranges from central roles to fundamental but hidden roles as simple co-factors in metabolic mechanisms [39]. However, the decrease in chlorophyll content and the increase in Mg⁺⁺ observed in the leaves of the infected plant would suggest that the infection would cause the degradation of “chlorophyll a” by forcing the plant to absorb more Mg⁺⁺ in an attempt to recover/produce the base amount of chlorophyll.

The chlorophyll content also decreased in tomato stems of the infected samples (Figure 5), whereas the emission patterns of both Mg⁺⁺ and C increased slightly for the infected sample with respect to the control (Figure 6). The yellowing of leaves is a non-specific symptom of disease caused by limitations on the availability of micro and macro nutrients, possibly due to attacks by phytophages, pathogenic fungi and viruses. In the case

of viral infections, this symptom is often associated with a reprogramming of the expression of key players in chlorophyll biosynthesis. It is now well established that viral infection induces the widespread down regulation of genes involved in chlorophyll biosynthesis. Among these, the expression of Mg-chelatase genes has been shown to be reduced in several combinations of plant viruses, such as cucumber mosaic virus in co-infection with CMV satellite Y in several plant species [40], and stripe virus in rice [41]. Our preliminary result of a reduced level of Mg^{++} ions in infected tissues is thus expected, as the incorporation of Mg^{++} ions into protein complexes is limited. Furthermore, Pool et al. [42] found that infection with *M. incognita* increased the C concentration in cowpea shoots and enhanced root biomass slightly. The presence of nematodes did not affect microbial biomass, but significantly changed the allocation of the photosynthate. Recent studies carried out on transgenic tobacco plants have shown a lower leaf starch and accumulation of soluble sugars as a result of an altered metabolism of C (lower leaf starch and accumulation of soluble sugars) and N (higher amounts of amino acids and soluble proteins). These results are in agreement with the thioredoxin (Trx)-mediated activation of the N metabolism at the expense of carbohydrates, as this is related to photosynthesis processes [43]. In conclusion, the decrease in chlorophyll content and the increase in Mg^{++} measured in the stems of infected plants is similar to those observed for the leaves.

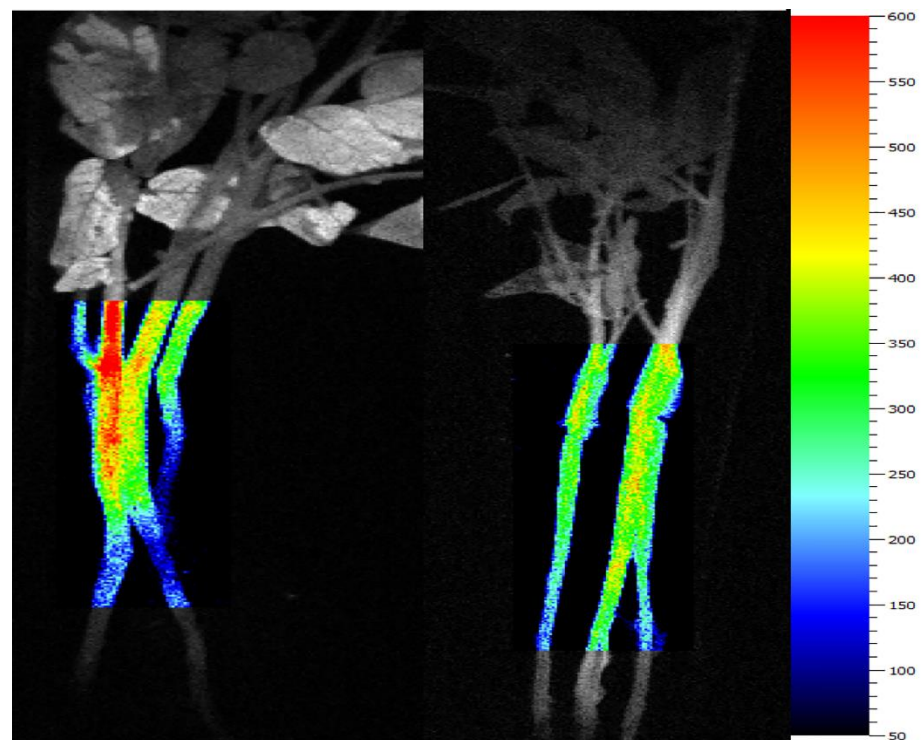


Figure 5. Fluorescence images (F_m measurements) of tomato stems of control plants (**left**) and plants with the root apparatus infected by *M. incognita* root (**right**).

As roots do not show chlorophyll emissions, only LIBS spectra were acquired on uninfected and *M. incognita*-infected root samples. The C emission line is very weak, and two Si I lines appear in the control sample, whereas the intensity of Mg^{++} lines was similar for both the control and infected roots (Figure 7). In this study, we used fresh leaves and roots, although the moisture content can greatly affect spectral features. In particular, as moisture content increases, many emission lines decrease markedly or even disappear.

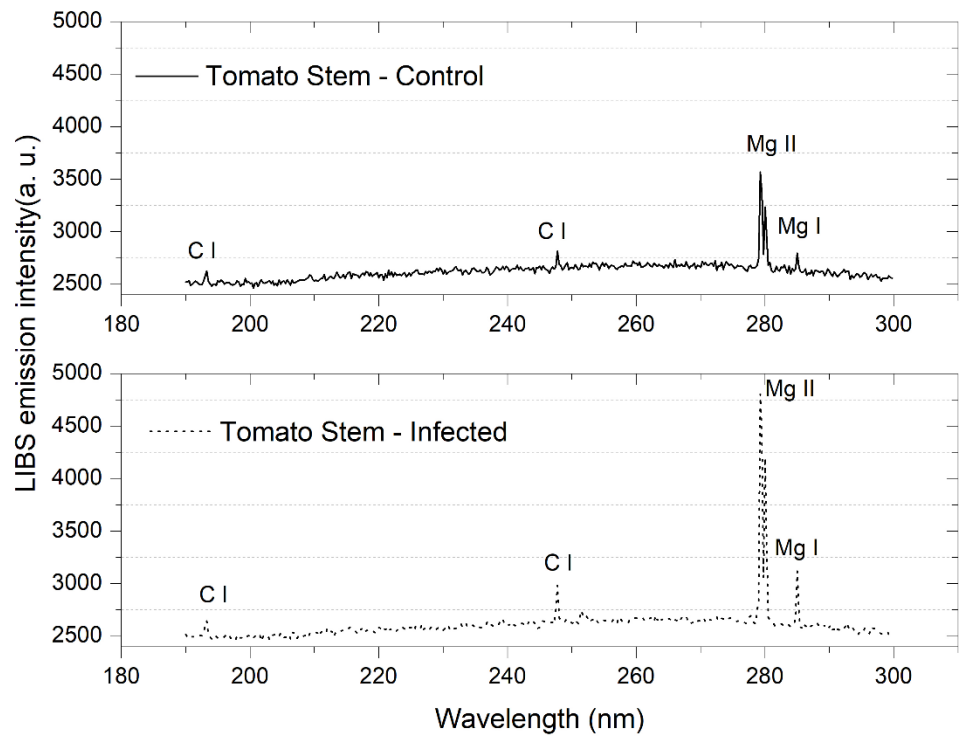


Figure 6. LIBS spectra of tomato stems of control plants and plants with roots infected by *M. incognita*.

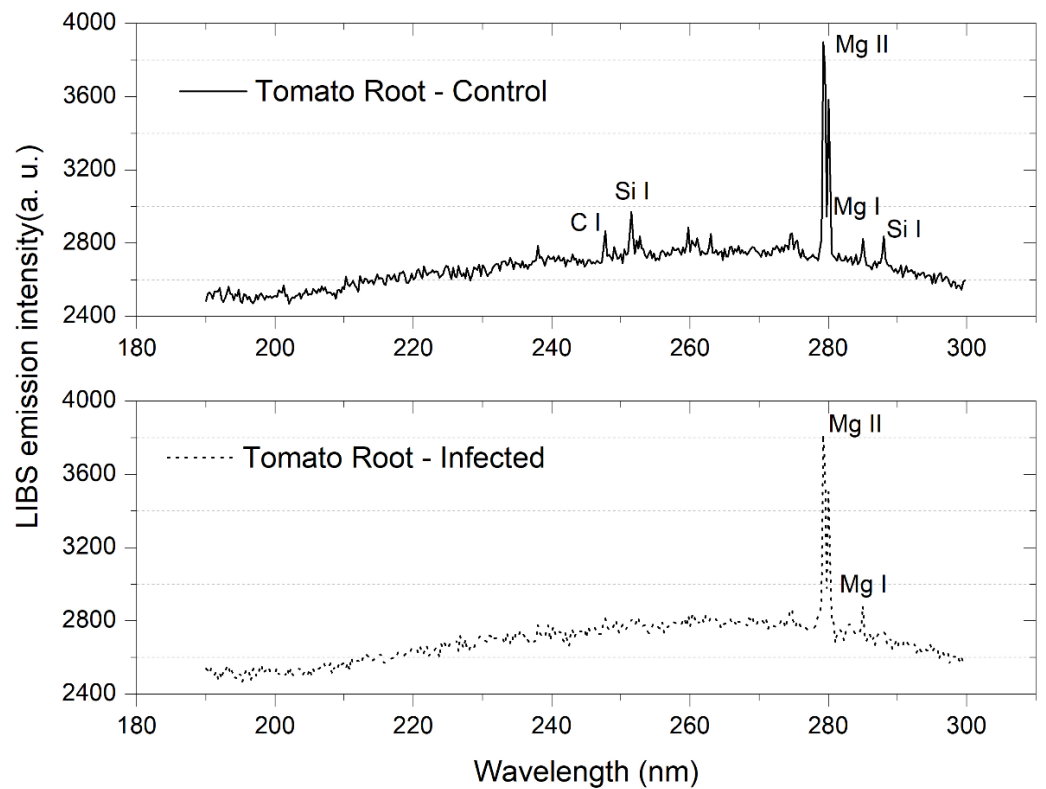


Figure 7. LIBS spectra of control and *M. incognita*-infected tomato roots.

3.2. Tobacco Leaves

Although in the case of tobacco plants infected by viruses, the reduction in chlorophyll is quite well supported by the literature, we applied CFI to tobacco leaves infected with CymRSV in order to confirm by this technique the symptoms clearly visible to the naked eye.

Some regions of the leaf showed clear deficiencies due to the deterioration of chlorophyll (Figure 8). In particular, the blue parts in the image confirmed the presence of chlorotic areas, which indicated that the disease had generated a condition in which the leaves, or part of them, have an altered content of chlorophyll.

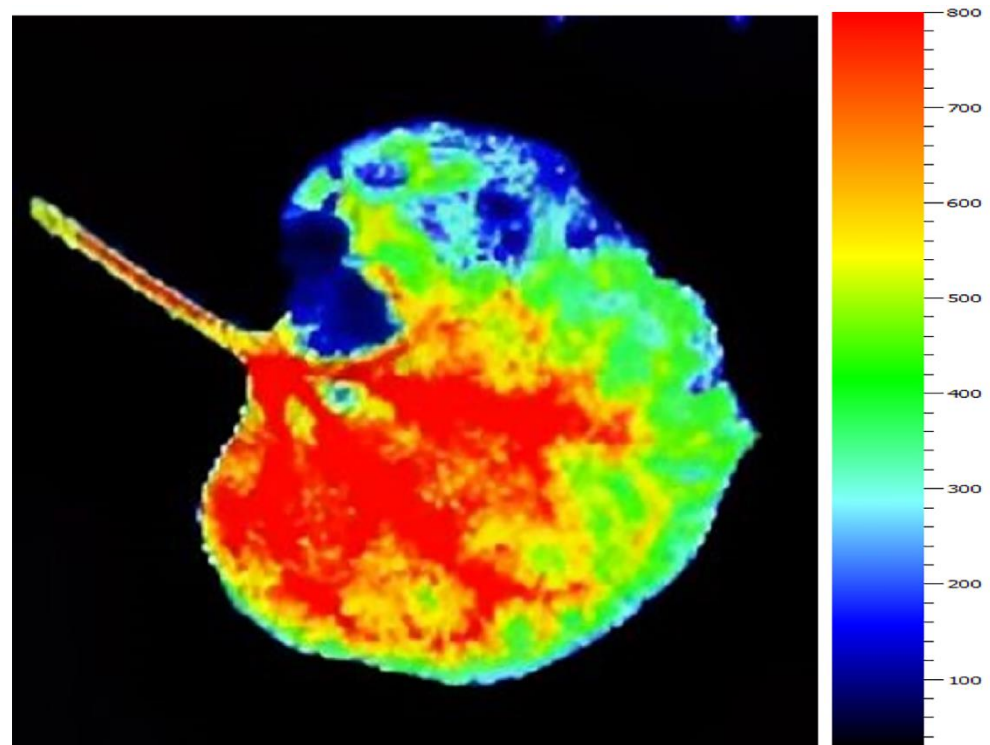


Figure 8. Fluorescence image of an infected tobacco leaf. False-blue color spots indicate where a chlorophyll deficiency is present.

The LIBS spectra of tobacco leaves (Figure 9) showed that, with respect to the control, the emission line intensities of C increased and those of Mg^{++} decreased in the infected sample. In this regard, it was shown that a specific mechanism of defense to diseases enhanced by Mg^{++} included the increased resistance of tissues to degradation by pectolytic enzymes of bacterial soft rotting pathogens [44].

A novel approach based on LIBS analysis was proposed by Peng et al. [22] to discriminate between tobacco leaves infected by the mosaic virus (TMV) and healthy leaves. The application of the partial least square discriminant analysis (PLS-DA) model to LIBS spectral data acquired on both fresh and dried pelletized leaves only provided good classification in the case of dried leaves. Apparently, the moisture content in fresh leaves worsened the stability of analysis, resulting in a detrimental effect on classification. However, when the SVM approach was used, the negative effect of moisture was eliminated, and the classification results were improved.

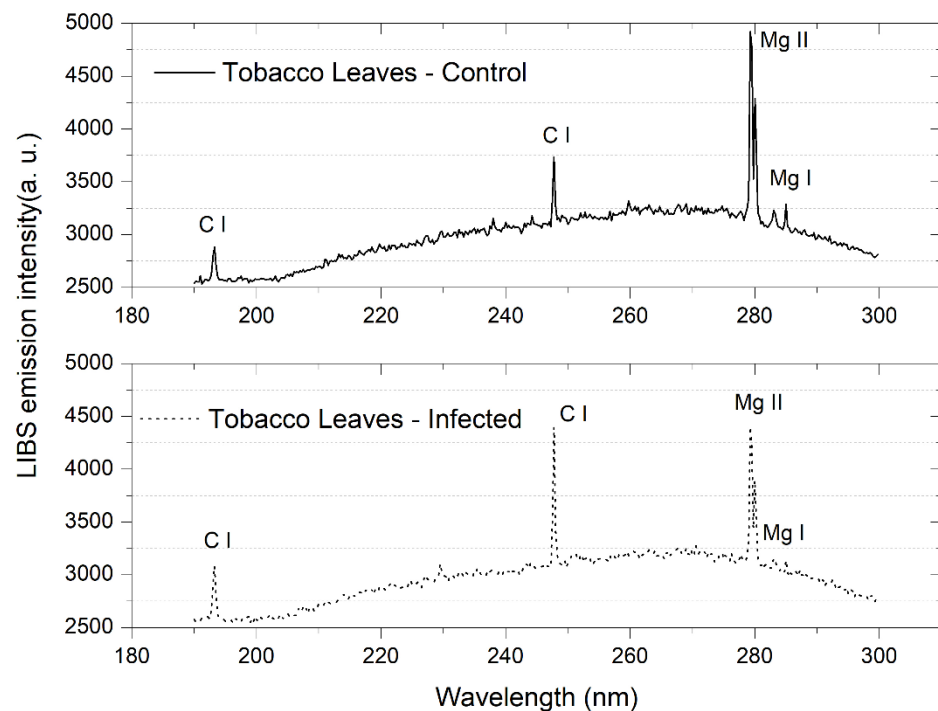


Figure 9. LIBS spectra of control and infected tobacco leaves.

3.3. Multivariate Analysis

The number of PCs used in the training was representative of 95% of the total variance of the system. The tests conducted on the dataset showed that the best performance was achieved using the KNN (euclidean with $k = 1$) and SVM (linear) classifiers. The results of the LOOCV were:

Tomato stems—KNN with 3PCs: 100% accuracy, 100% precision and 100% sensitivity;

Tomato roots—SVM with 2PCs: 52.4% accuracy, 50% precision and 50% sensitivity;

Tomato leaves—SVM with 4PCs: 84.2% accuracy, 88.9% precision and 80% sensitivity;

Tobacco leaves—SVM with 3PCs: 94.4% accuracy, 91.7% precision and 100% sensitivity.

These results indicate that the analysis of tomato stems shows the greatest potential for setting up a protocol to differentiate between healthy and infected samples by in vivo, direct, and no sample pre-treatment measurements. The classification based on the use of tomato roots was very close to 50%, which indicates a complete randomness of related data, whereas a better accuracy, i.e., 84.2%, was achieved based on tomato leaves data. These results may have been influenced by several factors, such as homogeneity, stress, humidity, hardness, etc., which would result in them being more relevant for roots. In this case, it would be necessary to carry out some pre-treatment of the samples in order to reduce the variance attributed to factors not related to the disease's condition. Furthermore, the machine learning tests confirm that only the stem data from direct measurements have the potential to be separated without the use of averages. For tobacco leaves, the accuracy was 94.4%, which also suggests a good potential for the development of a differentiation model.

4. Conclusions

In the current situation of climate change, in which abiotic and biotic stresses generate enormous problems for crop plants, growth and production, techniques and methods that can provide accurate and repeatable results on the state of host plants attacked by pathogens are highly expected to offer new possibilities for use, especially in precision agriculture. In particular, chemical analytical data acquired by portable equipment, combined with biochemical methods, would allow for real-time evaluations and fast and concrete interventions regarding plant diseases. Currently, most of the screening on the possible

reactions of different genotypes of tomato to different species and pathotypes of RKNs is based on molecular biology and the use of biochemical and epigenetic procedures that cannot be replicated for large numbers of samples and require a long time.

In this work, we have shown that the combined use of advanced biochemical (CFI) and spectroscopic (LIBS) techniques was very promising in the evaluation of two relevant plant diseases, i.e., a nematode infection of tomato and a virus infection of tobacco. In particular, the levels of chlorophyll in the leaves and stems of tomato plants and the leaves of tobacco plants measured by fluorescence imaging, and the levels of C and Mg⁺⁺ in various tomato organs and tobacco leaves measured by LIBS, have been shown to be able to discriminate satisfactorily between control (non-infected) and infected plants, and provide some insight on the underlying mechanisms of plant defense against nematodes and viruses. Thus, significant attention should be given to the underutilized management of Mg⁺⁺ nutrition, with respect to other cations, as a promising tool for plant disease control.

In conclusion, the adoption of LIBS with a timely reading of spectra in early diagnosis protocols can help prevent destructive viral infection outbreaks, especially with the aid of image processing by artificial intelligence and also in the case of identifying the pathogen by sequence-specific and metagenomic techniques. Furthermore, the LIBS technique has the advantage of being fast, and the availability of portable devices allows for its use directly in the field, thereby replacing long and complex laboratory analyses.

Author Contributions: Conceptualization, P.L. and G.S.S.; data curation, P.L., A.R.L.C., B.S.M. and G.S.S.; methodology, P.L., A.R.L.C., B.S.M. and G.S.S.; viral inoculation V.P.; formal analysis, P.L., A.R.L.C., B.S.M., G.N. and G.S.S.; investigation, P.L., A.R.L.C., B.S.M. and G.S.S.; writing—original draft preparation, G.S.S. and P.L.; writing—review and editing, P.L., V.P., A.R.L.C., B.S.M., G.N., O.D.P. and G.S.S. All authors have read and agreed to the published version of the manuscript.

Funding: This research received no external funding.

Institutional Review Board Statement: Not applicable.

Informed Consent Statement: Not applicable.

Data Availability Statement: Not applicable.

Conflicts of Interest: The authors declare no conflict of interest.

References

1. Vandvik, V.; Skarpaas, O.; Klanderud, K.; Telford, R.J.; Halbritter, H.; Goldberg, D.E. Biotic rescaling reveals importance of species interactions for variation in biodiversity responses to climate change. *Proc. Natl. Acad. Sci. USA* **2020**, *117*, 22858–22865. [[CrossRef](#)] [[PubMed](#)]
2. Abad, P.; Gouzy, J.; Aury, J.M.; Castagnone-Sereno, P.; Danchin, E.G.; Deleury, E.; Perfus-Barbeoch, L.; Anthouard, V.; Artiguenave, F.; Blok, V.C.; et al. Genome sequence of the metazoan plant-parasitic nematode *Meloidogyne incognita*. *Nat. Biotechnol.* **2008**, *26*, 909–915. [[CrossRef](#)] [[PubMed](#)]
3. Leonetti, P.; Accotto, G.P.; Hanafy, M.S.; Pantaleo, V. Viruses and phytoparasitic nematodes of *Cicer A. L.*: Biotechnological approaches in interaction studies for sustainable control. *Front. Plant Sci.* **2018**, *9*, 319. [[CrossRef](#)] [[PubMed](#)]
4. Lovey, S.; Bird, F. The influence of nematodes on photosynthesis in tomato plants. *Physiol. Plant Pathol.* **1973**, *3*, 525–529. [[CrossRef](#)]
5. Fujimoto, T.; Abe, H.; Mizukubo, T.; Seo, S. Phytol, a Constituent of Chlorophyll, Induces Root-Knot Nematode Resistance in *Arabidopsis* via the Ethylene Signaling Pathway. *Mol. Plant Microbe Interact.* **2021**, *34*, 279–285. [[CrossRef](#)]
6. Alon, D.M.; Hak, H.; Bornstein, M.; Pines, G.; Spiegelman, Z. Differential Detection of the Tobamoviruses Tomato Mosaic Virus (ToMV) and Tomato Brown Rugose Fruit Virus (ToBRFV) Using CRISPR-Cas12a. *Plants* **2021**, *10*, 1256. [[CrossRef](#)]
7. Singh, V.; Sharma, N.; Singh, S. A review of imaging techniques for plant disease detection. *Artif. Intell. Agric.* **2020**, *4*, 229–242. [[CrossRef](#)]
8. Leonetti, P.; Ghasemzadeh, A.; Consiglio, A.; Gursinsky, T.; Behrens, S.-E.; Pantaleo, V. Endogenous activated small interfering RNAs in virus-infected Brassicaceae crops show a common host gene-silencing pattern affecting photosynthesis and stress response. *New Phytol.* **2021**, *229*, 1650–1664. [[CrossRef](#)]
9. Grishina, A.; Sherstneva, O.; Grinberg, M.; Zdobnova, T.; Ageyeva, M.; Khlopkov, A.; Sukhov, V.; Brilkina, A.; Vodeneev, V. Pre-Symptomatic Detection of Viral Infection in Tobacco Leaves Using PAM Fluorometry. *Plants* **2021**, *10*, 2782. [[CrossRef](#)]
10. Sankaran, S.; Mishra, A.; Ehsani, R.; Davis, C. A review of advance techniques for detecting plant diseases. *Comput. Electron. Agric.* **2010**, *72*, 1–13. [[CrossRef](#)]

11. Tauseef, A.; Khalilullah, A.; Uddin, I. Role of MgO nanoparticles in the suppression of *Meloidogyne incognita*, infecting cowpea and improvement in plant growth and physiology. *Exp. Parasitol.* **2021**, *220*, 108045. [[CrossRef](#)] [[PubMed](#)]
12. Brouwer, S.M.; Lindqvist-Reis, P.; Persson, D.P.; Marttila, S.; Grenville-Briggs, L.J.; Andreasson, E. Visualising the ionome in resistant and susceptible plant-pathogen interactions. *Plant J.* **2021**, *108*, 870–885. [[CrossRef](#)] [[PubMed](#)]
13. Molinari, S.; Akbarimotlagh, M.; Leonetti, P. Tomato root colonization by exogenously inoculated arbuscular mycorrhizal fungi induces resistance against Root-Knot Nematodes in a dose-dependent manner. *Int. J. Mol. Sci.* **2022**, *23*, 8920. [[CrossRef](#)] [[PubMed](#)]
14. Senesi, G.S.; Harmon, R.S.; Hark, R. Field-portable and handheld laser-induced breakdown spectroscopy: Historical review, current status and future prospects. *Spectrochim. Acta Part B* **2021**, *175*, 106013. [[CrossRef](#)]
15. Kaiser, J.; Novotny, K.; Martin, M.Z.; Hrdlicka, A.; Malina, R.; Hartl, M.; Adam, V.; Kizek, R. Trace elemental analysis by laser-induced breakdown spectroscopy biological applications. *Surf. Sci. Rep.* **2012**, *67*, 233–243. [[CrossRef](#)]
16. Peng, J.; Liu, F.; Zhou, F.; Song, K.; Zhang, C.; Ye, L.; He, Y. Challenging applications for multi-element analysis by laser-induced breakdown spectroscopy in agriculture: A review. *TrAC Trends Anal. Chem.* **2016**, *85*, 260–272. [[CrossRef](#)]
17. Markiewicz-Keszycka, M.; Cama-Moncunill, X.; Casado-Gavaldà, M.P.; Dixit, Y.; Cama-Moncunill, R.; Cullen, P.J.; Sullivan, C. Laser-induced breakdown spectroscopy (LIBS) for food analysis: A review. *Trends Food Sci. Technol.* **2017**, *65*, 80–93. [[CrossRef](#)]
18. de Carvalho, G.G.A.; Braga Bueno Guerra, M.; Adame, A.; Seimi Nomura, C.; Oliveira, P.V.; de Carvalho, H.W.P.; Santos, D., Jr.; Nunes, L.C.; Krug, F.J. Recent advances in LIBS and XRF for the analysis of plants. *J. Anal. At. Spectrom.* **2018**, *33*, 919–944. [[CrossRef](#)]
19. Senesi, G.S.; Cabral, J.; Menegatti, C.R.; Marangoni, B.; Nicolodelli, G. Recent advances and future trends in LIBS applications to agricultural materials and their food derivatives: An overview of developments in the last decade (2010–2019). Part II. Crop plants and their food derivatives. *TrAC Trends Anal. Chem.* **2019**, *118*, 453–469. [[CrossRef](#)]
20. Pereira, F.M.V.; Milori, D.M.B.P.; Venancio, A.L.; de Russo, M.S.T.; Martins, P.K.; Freitas-Astúa, J. Evaluation of the effects of *Candidatus Liberibacter asiaticus* on inoculated citrus plants using laser-induced breakdown spectroscopy (LIBS) and chemometrics tools. *Talanta* **2010**, *83*, 351–356. [[CrossRef](#)]
21. Sankaran, S.; Ehsani, R.; Morgan, K.T. Detection of anomalies in citrus leaves using laser-induced breakdown spectroscopy (LIBS). *Appl. Spectrosc.* **2015**, *69*, 913–919. [[CrossRef](#)] [[PubMed](#)]
22. Peng, J.; Song, K.; Zhu, H.; Kong, W.; Liu, F.; Shen, T.; He, Y. Fast detection of tobacco mosaic virus infected tobacco using laser-induced breakdown spectroscopy. *Sci. Rep.* **2017**, *7*, 44551. [[CrossRef](#)] [[PubMed](#)]
23. Ranulfi, A.C.; Senesi, G.S.; Caetano, J.B.; Meyer, M.C.; Magalhaes, A.B.; Villas-Boas, P.R.; Milori, D.M.B.P. Nutritional characterization of healthy and *Aphelenchoides besseyi* infected soybean leaves by laser-induced breakdown spectroscopy (LIBS). *Microchem. J.* **2018**, *141*, 118–126. [[CrossRef](#)]
24. Molinari, S.; Leonetti, P. Bio-control agents activate plant immune response and prime susceptible tomato against root-knot nematodes. *PLoS ONE* **2019**, *14*, e0213230.
25. Molinari, S.; Fanelli, E.; Leonetti, P. Expression of tomato salicylic acid (SA)-responsive pathogenesis-related genes in Mi-1-mediated and SA-induced resistance to root-knot nematodes. *Mol. Plant Pathol.* **2014**, *15*, 255–264. [[CrossRef](#)] [[PubMed](#)]
26. Byrd, D.W.; Kirkpatrick, T., Jr.; Barker, K.R. An improved technique for clearing and staining plant tissue for detection of nematodes. *J. Nematol.* **1983**, *15*, 142–143.
27. Menegatti, C.R.; Nicolodelli, G.; Senesi, G.S.; Silva, O.A.; Filho, H.J.I.; Villas-Boas, P.R.; Marangoni, B.S.; Milori, D.M.B.P. Semiquantitative analysis of mercury in landfill leachates using double-pulse laser-induced breakdown spectroscopy. *Appl. Opt.* **2017**, *56*, 3730–3735. [[CrossRef](#)]
28. Marangoni, B.S.; Silva, K.S.G.; Nicolodelli, G.; Senesi, G.S.; Cabral, J.S.; Villas-Boas, P.R.; Silva, C.S.; Teixeira, P.C.; Nogueira, A.R.A.; Benites, V.M.; et al. Phosphorous quantification in fertilizers using laser induced breakdown spectroscopy (LIBS): A methodology of analysis to correct physical matrix effects. *Anal. Methods* **2016**, *8*, 78–82. [[CrossRef](#)]
29. Larios, G.; Ribeiro, M.; Arruda, C.; Oliveira, S.L.; Canassa, T.; Baker, M.J.; Marangoni, B.S.; Ramos, C.; Cena, C. A new strategy for canine visceral leishmaniasis diagnosis based on FTIR spectroscopy and machine learning. *J. Biophotonics* **2021**, *14*, e202100141. [[CrossRef](#)]
30. Allegretta, I.; Marangoni, B.S.; Manzari, P.; Porfido, C.; Terzano, R.; De Pascale, O.; Senesi, G.S. Macro-classification of meteorites by portable energy dispersive X-ray fluorescence spectroscopy (pED-XRF), principal component analysis (PCA) and machine learning algorithms. *Talanta* **2020**, *212*, 120785. [[CrossRef](#)]
31. Porra, R.J.; Thompson, W.A.; Kriedemann, P.E. Determination of accurate extinction coefficients and simultaneous equations for assaying chlorophylls a and b extracted with four different solvents: Verification of the concentration of chlorophyll standards by atomic absorption spectroscopy. *Biochim. Biophys. Acta* **1989**, *975*, 384–394. [[CrossRef](#)]
32. Melakeberhan, H.; Ferris, H. Impact of *Meloidogyne incognita* on Physiological Efficiency of *Vitis vinifera*. *J. Nematol.* **1989**, *21*, 74–80. [[PubMed](#)]
33. Lu, P.; Davis, R.F.; Kemerait, R.C.; van Iersel, M.W.; Scherm, H. Physiological Effects of *Meloidogyne incognita* Infection on Cotton Genotypes with Differing Levels of Resistance in the Greenhouse. *J. Nematol.* **2014**, *46*, 352–359. [[PubMed](#)]
34. Udalova, Z.V.; Zinovieva, S.V. Effect of Salicylic Acid on the Oxidative and Photosynthetic Processes in Tomato Plants at Invasion with Root-Knot Nematode *Meloidogyne incognita* (Kofoid Et White, 1919) Chitwood, 1949. *Dokl. Biochem. Biophys.* **2019**, *488*, 350–353. [[CrossRef](#)]

35. Udalova, Z.V.; Folmanis, G.E.; Fedotov, M.A.; Pelgunova, L.A.; Krysanov, E.Y.; Khasanov, F.K.; Zinovieva, S.V. Effects of Silicon Nanoparticles on Photosynthetic Pigments and Biogenic Elements in Tomato Plants Infected with Root-Knot Nematode *Meloidogyne incognita*. *Dokl. Biochem. Biophys.* **2020**, *495*, 329–333. [[CrossRef](#)]
36. Niyogi, K.K. Photoprotection revisited: Genetic and molecular approaches. *Annu. Rev. Plant Physiol. Plant Mol. Biol.* **1999**, *50*, 333–359. [[CrossRef](#)]
37. Labudda, M.; Rózańska, E.; Czarnocka, W.; Sobczak, M.; Dzik, J.M. Systemic changes in photosynthesis and reactive oxygen species homeostasis in shoots of *Arabidopsis thaliana* infected with the beet cyst nematode *Heterodera schachtii*. *Mol. Plant Pathol.* **2018**, *19*, 1690–1704. [[CrossRef](#)] [[PubMed](#)]
38. NIST Database. 2022. Available online: <https://physics.nist.gov/PhysRefData/ASD/LIBS> (accessed on 16 May 2022).
39. Luo, T.; Fan, T.; Liu, Y.; Rothbart, M.; Yu, J.; Zhou, S.; Grimm, B.; Luo, M. Thioredoxin redox regulates ATPase activity of magnesium chelatase CHLI subunit and modulates redox-mediated signaling in tetrapyrrole biosynthesis and homeostasis of reactive oxygen species in pea plants. *Plant Physiol.* **2012**, *159*, 118–130. [[CrossRef](#)]
40. Shimura, H.; Pantaleo, V.; Ishihara, T.; Myojo, N.; Inaba, J.; Sueda, K.; Burguán, J.; Masuta, C. A viral satellite RNA induces yellow symptoms on tobacco by targeting a gene involved in chlorophyll biosynthesis using the RNA silencing machinery. *PLoS Pathog.* **2011**, *7*, e1002021. [[CrossRef](#)]
41. Wang, B.; Hajano, J.-U.-D.; Ren, Y.; Lu, C.; Wang, X. iTRAQ-based quantitative proteomics analysis of rice leaves infected by *Rice stripe virus* reveals several proteins involved in symptom formation. *Virology*. **2015**, *12*, 99. [[CrossRef](#)]
42. Poll, J.; Marhan, S.; Haase, S.; Hallmann, J.; Kandeler, E.; Ruess, L. Low amounts of herbivory by root-knot nematodes affect microbial community dynamics and carbon allocation in the rhizosphere. *FEMS Microbiol. Ecol.* **2007**, *62*, 268–279. [[CrossRef](#)] [[PubMed](#)]
43. Ancín, M.; Larraya, L.; Florez-Sarasa, I.; Bénard, C.; Fernández-San Millán, A.; Veramendi, J.; Gibon, Y.; Fernie, A.R.; Aranjuelo, I.; Farran, I. Overexpression of thioredoxin m in chloroplasts alters carbon and nitrogen partitioning in tobacco. *J. Exp. Bot.* **2021**, *72*, 4949–4964. [[CrossRef](#)] [[PubMed](#)]
44. Huber, D.M.; Jones, J.B. The role of magnesium in plant disease. *Plant Soil* **2013**, *368*, 73–85. [[CrossRef](#)]